Japanese Journal of Applied Physics **52** (2013) 10MB08 **REGULAR PAPER**
http://dx.doi.org/**10.7567/JJAP.52.10MB08**

Improvement in Cycle Performance by Suppression of Surface Reaction between Electrolyte and LiV_3O_8 Electrode Using Gel Polymer Electrolyte

Jung Min Seo[1], Jee Ho Yom[1], Woo Young Yoon[1]*, and Dong Won Kim[2]

[1]*Department of Materials Science and Engineering, Korea University, Seoul 136-701, Republic of Korea*
[2]*Department of Chemical Engineering, Hanyang University, Seoul 133-791, Republic of Korea*
E-mail: wyyoon@korea.ac.kr

Received December 3, 2012; accepted July 20, 2013; published online October 21, 2013

Amorphous lithium trivanadate (LVO) exhibits a higher capacity than crystalline LVO. However, products are generated from the reaction between the surface of an amorphous LVO electrode and the surrounding electrolyte during charging and discharging. The continuous reaction between the electrode surface and surrounding electrolyte was inhibited using a gel-polymer electrolyte (GPE) instead of a conventional liquid electrolyte. After 100 cycles, the GPE-based cell shows 54% of capacity retention, which was 9% higher capacity retention than that of the conventional liquid electrolyte cell. The GPE is prepared as Kynar 2801 polymer and the charge and discharge performances of the cell were measured using a standard battery cycling test at a 0.5 C-rate and 1.5–4.0 V cut off voltage. The morphologies of the electrode surfaces and the various products formed on the electrode surfaces during the reaction were analyzed using scanning electron microscopy (SEM) and energy dispersive X-ray (EDX) spectroscopy, respectively.

1. Introduction

Studies on high-capacity batteries for electric vehicles and energy-storage systems are currently in progress.[1–8] Lithium trivanadate (LVO) is a well-known cathode material that exhibits a higher capacity than lithium cobalt oxide (LCO) does. The theoretical capacity of LVO is 280 mAh/g, and many studies have been performed to increase LVO capacity.[2–6] Although amorphous LVO exhibits a capacity 1.5 times higher than that of crystalline LVO,[7,8] it also exhibits sudden capacity fading during charging and discharging. Such fading is not exhibited during cycling of crystalline LVO. The capacity fading exhibited by crystalline LVO is due to the change in volume of the electrode and the dissolution of vanadium into the surrounding electrolyte during the cycling.[9,10] In addition, the surface of an amorphous LVO electrode undergoes a continuous side reaction with the surrounding electrolyte, resulting in decreased capacity.[11] Li metal is used as an anode material because LVO is a nonlithiated cathode material. Li metal exhibits high theoretical capacity of 3860 mAh/g; however, it also exhibits weak cycle properties because of dendrite formation during charging and discharging. In our previous study, we found that Li powder suppressed dendrite formation during cycling.[12,13]

Recently, many studies have focused on improving the safety of lithium ion batteries by using a gel polymer electrolyte (GPE).[14–19] Although the main disadvantage of GPE is its low ionic conductivity, it is much safer than liquid electrolyte because it prevents the explosions that commonly occur when liquid electrolyte leaks from lithium ion batteries. Moreover, relevant research indicates that GPE stabilizes electrode surfaces, helping to improve the capacity retention of electrodes.[20,21]

In the present study, liquid electrolyte was replaced with GPE to inhibit the reaction between the LVO cathode surface and the electrolyte. This is the first report for Li metal–amorphous LVO cell with GPE. The capacity retention of the GPE-based cell was analyzed to determine by how much it would improve compared with a liquid-electrolyte-based cell.

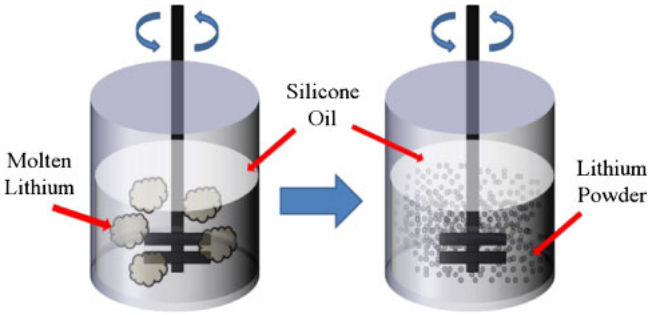

Fig. 1. (Color online) Schematic diagram of the DET apparatus.

2. Experimental Procedure

Li powders were prepared using the droplet emulsion technique (DET). Figure 1 shows a schematic diagram of the DET apparatus. Silicone oil (Shin-Etsu) was used as an emulsifier to prepare Li powder. Melted lithium was added to the oil that had been preheated to the melting point of lithium. The silicone oil and molten lithium mixture was stirred using a trimmer at 25,000 rpm to produce an emulsion. The stirred emulsion was then cooled to room temperature, to form spherical Li powder particles. The Li powder particles were rinsed using hexane to separate them from the oil. As shown in Fig. 2, a porous lithium powder electrode was prepared by compacting the lithium powder with a press. Amorphous LVO was prepared by stirring together 3 mol of V_2O_5 (Aldrich) and a solution containing 2 mole of lithium hydroxide at 70 °C for 3 days.[8]

The LVO electrode was fabricated by the tape-casting method for electrochemical analysis. A slurry containing 80 wt % LVO, 15 wt % Ketjenblack as a conductive agent, and 5 wt % sodium carboxymethyl cellulose (Na-CMC) as a binder was tape-cast onto an Al-foil. The cast electrode was dried in a vacuum oven at 120 °C for 1 h. Elctrochemical characterization were performance using coin cell (CR2032). A Celgard® 2300 separator was used to produce a cell with a liquid electrolyte but was not used to produce the cell with the gel polymer. A liquid electrolyte mixture

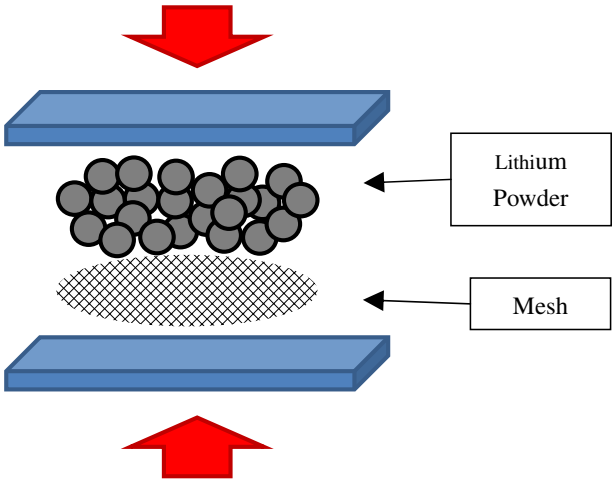

Fig. 2. (Color online) Schematic diagram of the press used to fabricate the lithium-powder electrode.

was prepared by dissolving 1 M $LiPF_6$ in a mixture of ethylene carbonate (EC), dimethyl carbonate (DMC), and ethyl methyl carbonate (EMC) in a volume ratio of 1 : 1 : 1 (Techno Semichem). Poly(vinylidene difluoride)–hexafluoropropylene (PVdF–HFP)-copolymer was used as the GPE. GPE was produced by using Kynar 2801. Kynar 2801 was dissolved in acetone and stirred in 12 h. Dissolved Kynar 2801 has changed in film form through the casting method. The film was immersed in an electrolyte which makes gelation process. All the experiments were performed in an argon gas-filled glove box. The electrochemical experiments were performed at a constant current (0.5 C-rate), using a Wonatech WBCS 3000 instrument. The morphology of the electrode was observed through scanning electron microscopy (SEM) and energy dispersive X-ray spectroscopy (EDX). The charge and discharge processes are used to analysis the difference of the products and the cycle performance.

3. Results and Discussion

Figure 3 shows the initial shape of Li powder particles comprising the anode. The powder particles are initially spherical, as shown Fig. 3(a), and the spherical shape was preserved after 100 cycles in the liquid-electrolyte-based cell, as shown in Fig. 3(b). Figure 3(c) shows the lithium powder particles comprising the anode in the GPE-based cell after 100 cycles. Most of the powder particles also show initial spherical shape and some exhibit only small depressions after 100 charge/discharge cycles.

SEM images of the amorphous LVO electrode taken before cycling and after 100 cycles are shown in Fig. 4. The morphology of the electrode surface before cycling is shown in Fig. 4(a). The amorphous LVO exhibits no specific shape, and it is mixed well with Ketjenblack throughout the electrode surface. However, the surface exhibits significant change in shape after 100 cycles, as shown in Figs. 4(b) and 4(c). Numerous cracks had developed during cycling and, therefore, the active materials seemed to be exfoliated. However, GPE cell shows relatively less surface cracks and exfoliation than the liquid electrolyte cell. During cycling, the volume of the electrode changes because of lithiation and delithiation, and such change caused the cracking and

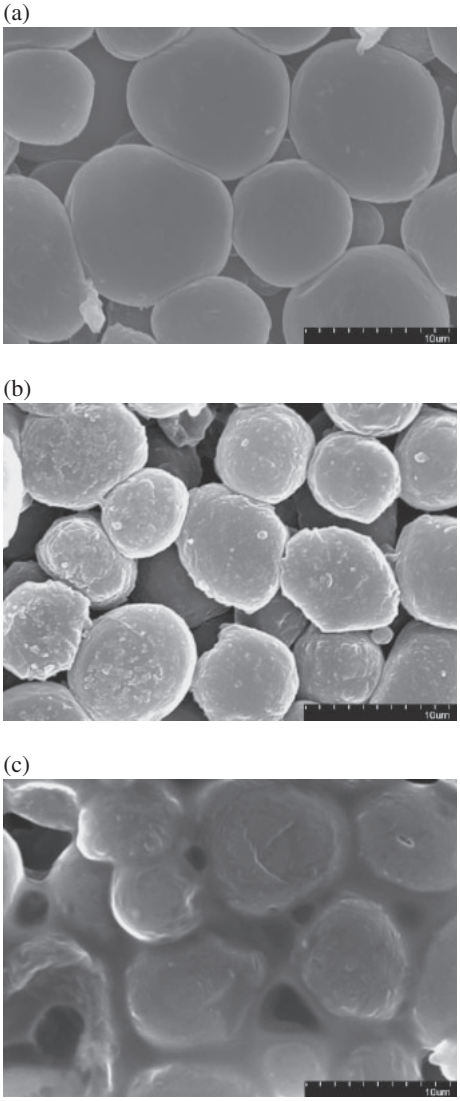

Fig. 3. The shapes of Li powder anodes after 100 cycles (a) in liquid-electrolyte-based cell and (b) in GPE-based cell.

exfoliation. Because of exfoliation, some electrode material could not participate in the electrochemical reaction. As a result, the LVO electrode exhibited capacity fading. This was observed for the electrodes in both the liquid electrolyte and GPE cells, and this may be one of the major causes of capacity fading of amorphous LVO electrode.

Figure 5 shows a high-resolution SEM image of the amorphous LVO electrode after 100 cycles. Figures 5(a) and 5(b) show the surfaces of the electrodes after cycling with the liquid electrolyte and GPE, respectively. Some reaction products were formed on the surface of the electrode cycled with the liquid electrolyte, and they can be seen in Fig. 5(a), on the other hand, no significant products were observed in GPE cell as shown in Fig. 5(b).

The surface reaction products were analyzed using EDX spectroscopy. Figures 6(a) and 6(b) show the ratios of the elements in the products formed on the surfaces of the both electrodes after 100 cycles with the liquid electrolyte and GPE, respectively. There are high ratios of fluorine in electrode cycled with the liquid electrolyte but no fluorine in the electrode cycled with GPE. A recent study has revealed that the reaction products Li_2O, Li_2CO_3, and LiF are

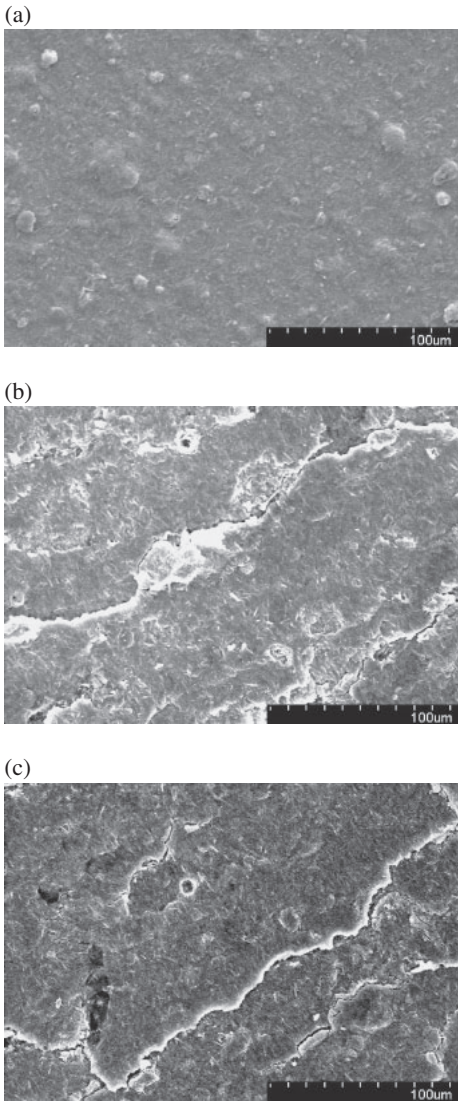

Fig. 4. SEM images of the surfaces of LVO electrodes (a) before cycling and after 100 cycles in (b) liquid-electrolyte-based cell and (c) GPE-based cell.

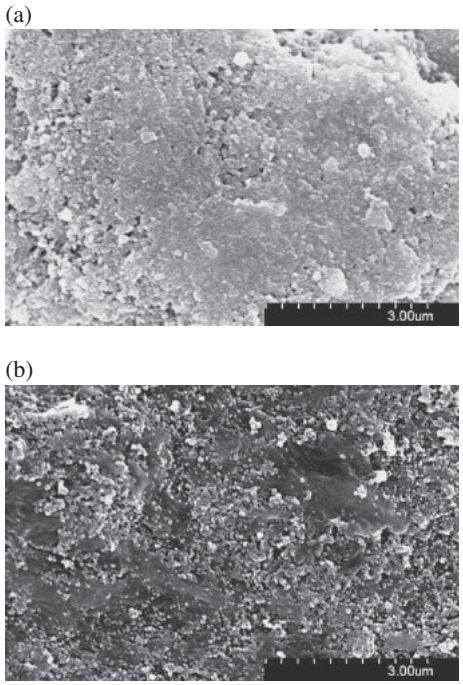

Fig. 5. High-resolution SEM images of amorphous LVO electrodes after 100 cycles. (a) Liquid electrolyte cell and (b) GPE cell.

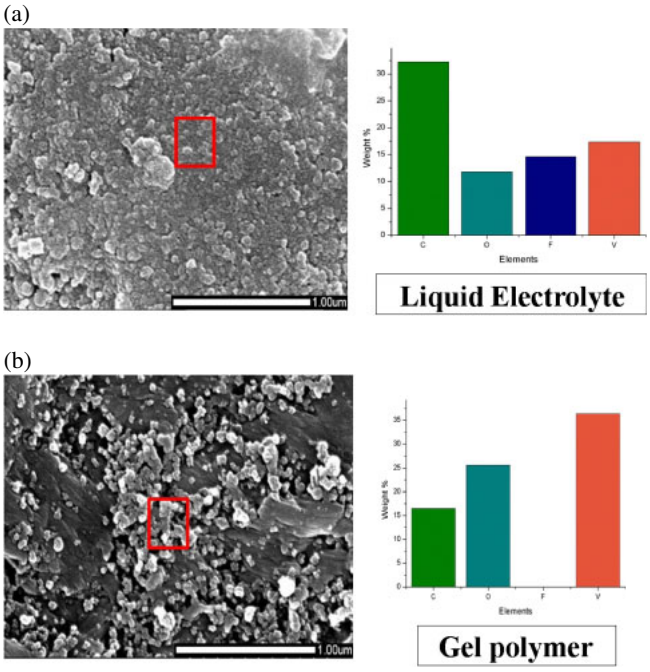

Fig. 6. (Color online) EDX spectroscopy of LVO surfaces after 100 cycles (a) liquid electrolyte cell and (b) GPE cell. Ratio and contents of elements found on LVO electrode surfaces are significantly different.

produced on the surface of LVO electrodes during cycling.[11] From the EDX data, it is obvious that reaction products were generated on the surface of the LVO electrode in liquid-electrolyte-based cell but reaction were not generated in GPE-based-cell. Figure 6 shows that the GPE had suppressed continuous reaction between the electrode surface and electrolyte in charge–discharge process.

Figure 7 shows the discharge capacities, measured at a 0.5 C-rate, plotted as a function of the number of cycles for the cells produced with liquid and gel polymer electrolytes. The initial capacity of the liquid-electrolyte-based cell is higher than that of the GPE-based cell. The discharge capacity of the liquid-electrolyte-based cell was 375 mAh/g during the first cycle, while that of the GPE-based cell was 345 mAh/g. However, as the number of cycles increased, the capacity of the liquid-electrolyte-based cell became lower than that of the GPE-based cell due to generation reaction products on the surface of liquid-electrolyte-based cell. The GPE-based cell exhibited better capacity retention and higher discharge capacity than the liquid-electrolyte-based cell after 40 cycles. Integration areas of two discharge capacity plots before 90 cycles, liquid-electrolyte-based cell shows 23955 mAh/g and it is larger than 23949 mAh/g of GPE-based cell. GPE-based cell had larger integration capacity (24145 mAh/g) than liquid-electrolyte-based cell (24133 mAh/g) after 91 cycles. After 100 cycles, the GPE-based cell exhibited a discharge capacity of 185 mAh/g, which is 54% of its initial discharge capacity, while the liquid-electrolyte-

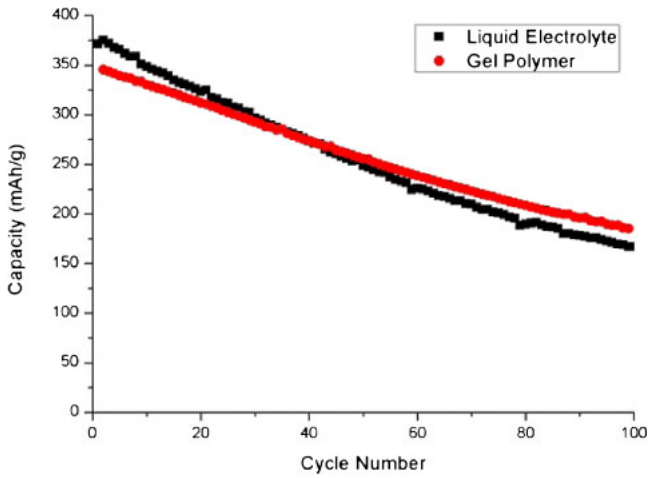

Fig. 7. (Color online) Cycling data for the liquid electrolyte and GPE cell measured at 0.5 C-rate.

based cell exhibited a discharge capacity of 167 mAh/g, which is only 45% of its initial discharge capacity. Because of the low ion conductivity of the GPE, the initial discharge capacity of the GPE-based cell was lower than that of the liquid-electrolyte-based cell. However, as shown in Figs. 4–6, the suppression of the reaction between the electrode surface and the surrounding electrolyte reduced the capacity fading of the GPE-based cell.

4. Conclusions

The amorphous Li metal–LVO cell exhibits a higher discharge capacity than the Li metal–crystalline LVO cell. However, it also exhibits high capacity fading during charging and discharging. The capacity fading of the amorphous LVO cell may due to the reaction between the surface of the amorphous LVO electrode and the surrounding electrolyte leading to cracking on the electrode surface, exfoliation of active materials from the surface of the collector electrode, and generation of products. The surface reaction was suppressed and cycle performance was improved using GPE. EDX data for the liquid-electrolyte-based and GPE-based cells measured after 100 cycles show a clear difference between the surface reactions of the two cells. As a result, the capacity retention rate improved by 9% in GPE-based cells. However, the exfoliation of active materials due to volume expansion of the amorphous LVO electrode remains a significant cause of capacity fading, though it reduced. Suppressing this volume expansion during cycling will enhance further the cycle performance of Li metal–amorphous LVO cells.

Acknowledgments

This study was supported by a grant (2011-0028757) from the National Research Foundation (NRF) of Korea funded by the Korean government (MEST). The surface of the electrode were observed using the Scanning electron microscope (SEM) located in the Korea Basic Science Institute Seoul Center.

1) L. Guo, W. Y. Yoon, and B. K. Kim: Electron. Mater. Lett. **8** (2012) 405.
2) D. K. Yun and W. Y. Yoon: Electron. Mater. Lett. **7** (2011) 221.
3) M. Dubarry, J. Gaubicher, D. Guyomard, O. Durupthy, N. Steunou, J. Livage, N. Dupre, and C. P. Grey: Chem. Mater. **17** (2005) 2276.
4) Y. M. Liu, X. C. Zhou, and Y. L. Guo: Mater. Chem. Phys. **114** (2009) 915.
5) A. M. Kannan and A. Manthiram: J. Power Sources **159** (2006) 1405.
6) L. Eriksson and B. Alm: Water Sci. Technol. **28** (1993) 203.
7) G. Pistoia and M. Pasquali: Prog. Batteries Sol. Cells **8** (1989) 143.
8) R. Tossici, R. Marassi, M. Berrettoni, S. Stizza, and G. Pistoia: Solid State Ionics **57** (1992) 227.
9) S. Jouanneau, A. L. La Salle, A. Verbaere, and D. Guyomard: J. Electrochem. Soc. **152** (2005) A1660.
10) S. Jouanneau, A. Verbaere, S. Lascaud, and D. Guyomard: Solid State Ionics **177** (2006) 311.
11) Q. Shi, R. Z. Hu, M. Q. Zeng, M. J. Dai, and M. Zhu: Electrochim. Acta **56** (2011) 9329.
12) J. S. Kim and W. Y. Yoon: Electrochim. Acta **50** (2004) 531.
13) I. W. Seong, C. H. Hong, B. K. Kim, and W. Y. Yoon: J. Power Sources **178** (2008) 769.
14) F. Yuan, H. Z. Chen, H. Y. Yang, H. Y. Li, and M. Wang: Mater. Chem. Phys. **89** (2005) 390.
15) W. Pu, X. He, L. Wang, C. Jiang, and C. Wan: J. Membrane Sci. **272** (2006) 11.
16) H. S. Kim, P. Periasamy, and S. I. Moon: J. Power Sources **141** (2005) 293.
17) N. T. Kalyana Sundaram and A. Subramania: J. Membrane Sci. **289** (2007) 1.
18) C. Y. Chiu, Y. J. Yen, S. W. Kuo, H. W. Chen, and F. C. Chang: Polymer **48** (2007) 1329.
19) X. L. Wang, A. Mei, M. Li, Y. H. Lin, and C. W. Nan: Solid State Ionics **177** (2006) 1287.
20) V. R. Koch, C. Nanjundiah, G. Battista Appetecchi, and B. Scrosati: J. Electrochem. Soc. **142** (1995) L116.
21) H. Matsumoto, M. Yanagida, K. Tanimoto, M. Nomura, Y. Kitagawa, and Y. Miyazaki: Chem. Lett. **29** (2000) 922.